

Optimal PMU placement for power system state estimation with random component outages



Xin Tai, Damián Marelli, Eduardo Rohr, Minyue Fu *

The School of Electrical Engineering and Computer Science, University of Newcastle, NSW 2308, Australia

ARTICLE INFO

Article history:

Received 19 April 2012

Received in revised form 30 January 2013

Accepted 2 February 2013

Available online 3 April 2013

Keywords:

Optimal PMU placement

State estimation

MAP estimation

Kalman filter

ABSTRACT

Phasor measurement units (PMUs) provide globally synchronized measurements of voltage and current phasors in real-time and at a high sampling rate. Hence, they permit improving the state estimation performance in power systems. In this paper we propose a novel method for optimal PMU placement in a power system suffering from random component outages (RCOs). In the proposed method, for a given RCO model, the optimal PMU locations are chosen to minimize the state estimation error covariance. We consider both static and dynamic state estimation. To reduce the complexity, the search for the optimal PMU locations is constrained to the set of locations guaranteeing topological observability. We present numerical results showing the application and scalability of our method using the IEEE 9-bus, 14-bus, 39-bus and 118-bus systems.

© 2013 Elsevier Ltd. All rights reserved.

1. Introduction

The fast penetration of renewable energy sources have generated increasing difficulties for reliable electric energy. Real-time dynamic monitoring, analysis, protection and control of energy management system (EMS) become necessary to combat the fluctuations caused by renewable power supply and fast load changes. State estimation (SE) technology, as a key EMS functionality, provides a real-time database of the state of the power system. Efficient and accurate SE is a prerequisite for the reliable operation of the EMS. After Schweppe and Wildes introduced the concept of SE in the field of power system in the early 1970s [1], many estimation methods have been proposed. In particular, static estimation, based on the least squares method, has been successfully applied in practice, for SE using the conventional supervisory control and data acquisition (SCADA) measurements. However, the low sampling rate and relatively low accuracy of SCADA measurements limit the reliability of SE. The development of phasor measurement units (PMUs) is extremely important in this context, since they permit a significant improvement of power system SE technology [2].

PMU devices have several crucial advantages over the conventional SCADA systems: (1) The sampling rate of PMU measurements (usually 30 measurements per second or more) is much higher than that of SCADA measurements (several seconds per measurement). This is important to enhance the monitoring and analysis of the dynamic behavior of power systems; (2) PMUs

provide synchronous measurements (via global synchronous time stamps), which can synchronize measurements from distant locations, so as to give a real-time picture of the whole power system; (3) A PMU can directly measure both the voltage phasor of the bus, where it is installed, and the current phasors of the branches linked to that bus. Hence, simple linear state estimation can be used, resulting in higher precision and faster calculation, in comparison with conventional nonlinear state estimation methods; (4) A PMU measurement has a much higher precision than that of a SCADA. If every bus of the power system is installed with a PMU, the EMS can be operated directly by the obtained measurements, without the need for SE. However, due to the expensive cost of PMU devices, as well as the limited communication channel bandwidth, it is impossible to install a PMU on every node of the power network. Hence, a smart selection of number and locations of PMU devices is an important problem.

In recent years, there has been a significant amount of research on the problem of optimal placement for PMUs. Generally speaking, these methods aim at minimizing the number of PMUs under various types of constraints, among which is the constraint that the whole system must be *topologically observable*. Roughly speaking, topological observability of a power system means that, at any time instant k , the whole state of the system can be uniquely determined from noise-free measurements obtained at the same time k . To deal with the PMU placement problem to guarantee topological observability, a number of stochastic search algorithms have been proposed, e.g., simulated annealing [3,4], genetic algorithm [5,6], non-dominated sorting genetic algorithm [7,8], Tabu search [9,10], binary search [11], iterated local search [12] and swarm optimization [13,14]. A number of deterministic search algorithms

* Corresponding author. Tel.: +61 2 4921 7730.

E-mail address: Minyue.Fu@newcastle.edu.au (M. Fu).

have also been proposed, e.g., integer programming [15–20] and quadratic programming [21,22]. In general, these algorithms yield a number of optimal solutions, i.e., there exist in general more than one PMU placement solutions that make the whole power system topologically observable with the same number of PMUs (e.g., our test shows that more than 2.5×10^4 different solutions can be obtained for the IEEE 118-bus system).

In order to refine the multiple optimal solutions obtained from the methods described above, a number of optimization criteria are available. One of them is the maximum measurement redundancy (MMR) criterion [5,23,22,13], which is used to maximize the total number of line current measurements for the given (minimum) number of PMUs. This method significantly reduces the number of PMU placements but does not yield a unique solution (e.g., 48 and 78 solutions are generated for the IEEE 39-bus and 118-bus systems, respectively). To resolve this problem, the authors of [24] consider dynamic state estimation and use the steady state Kalman filter state estimation error covariance to choose the optimal solution. While this approach leads to a unique solution, as we show in Section 5, this solution may no longer be optimal in the presence of random component outages (RCOs). For traditional power systems, RCO usually refers to power equipment failures (e.g., transition lines and transformers). In this paper, we extend this concept to include sensor failure and communication packet loss. We emphasize that RCO is a serious problem for PMUs, especially in real-time operations because measurement losses can be caused by (1) loss of global positions system (GPS) timing due to weather problems; (2) excessive communication delays; (3) outage in communication networks.

The occurrence of RCOs is considered in [25], where the optimal placement solution is chosen to maximize the probability of topological observability. RCO problems also have been considered in a deterministic way in many papers, e.g., [26,15,18,8,14,27]. In most of these papers, robust deterministic solutions of optimal PMU placement are proposed, in which backups of measurements are used to replace the lost measurements. However, we can not guarantee that the original measurements and the backup do not fail simultaneously, and the effectiveness of the backup data can be questionable in time-critical operations (e.g., in dealing with power failures).

Measurement placement methods in power systems usually consider two problems: (1) the improvement of the network observability and (2) the minimization of the errors in the estimates. In this paper we propose a new method to study the PMU placement problem based on two optimization criteria, i.e. topological observability guarantee and state estimation error covariance (EEC) minimization. A modified integer linear programming (ILP) method is proposed to generate all possible candidate PMU placement solutions to guarantee topological observability. Then we use the SE performance, i.e. EEC, as the optimization criterion to refine the candidate solutions. Also a more practical situation with RCOs occurring is considered. In the ideal case when RCOs do not occur, the proposed method searches for the solution which minimizes the norm of the EEC. The motivation for our criterion is that the covariance of the SE error in the power system is governed by the eigenvalues of the EEC. Since the norm of the EEC equals its largest eigenvalue, minimizing the norm is equivalent to minimizing the worst case, i.e., the largest estimation error in some sense. We apply this criterion in two scenarios, namely, static and dynamic estimations. In Static State Estimation (SSE), we estimate the state using some prior statistical information and available measurements. This is done using a maximum *a posteriori* criterion (MAP). On the other hand, in Dynamic State Estimation (DSE), the estimation is done using the statistics of the state at sample time k , conditioned on the measurements available up to time $k - 1$. This is done using a Kalman filter. DSE is considered in this paper be-

cause the measurements at adjacent sampling times are typically highly correlated due to the high sampling rate of PMUs, which is in large contrast to SCADA measurements (see more details in Section 2). In the presence of RCO, topological observability can not be guaranteed. The traditional static estimation algorithm, i.e., weighted least squares, will face numerical problem, whereas the proposed two kinds of estimators using previous statistical information can continue to provide good estimation.

When RCOs occur, the EEC becomes a stochastic matrix. In this situation, and in the case of SSE, a natural extension of the optimization criterion is to choose the placement such that the expected value of the norm of the EEC is minimized. On the other hand, in the case of DSE, this expected value is time-varying. Hence, the natural extension involves minimizing its asymptotic value. A difficulty in doing so is that, there is no simple expression to compute this asymptotic value. To get around this, we derive a sequence of upper and lower bounds on it. Using these bounding sequences, we derive an algorithm to find the optimal solution. The proposed algorithm is a sequential one in the sense that at each step it chooses a set of tighter bounds, it then eliminates, from the set of candidate solutions, those which are no longer candidates for the optimal solution, and it stops when the set of candidates has only one solution left. Our method is evaluated in the IEEE 9-bus test system. A unique optimal PMU placement solution is obtained for this test system. The experiments also show that, for the case of DSE, the optimal solution depends on the RCO rate.

However, there is still a problem of the bounding sequence algorithm above, i.e., when applied to a large size power system or using a relatively large number of steps, the proposed algorithm can make the calculation of the upper and lower bounds numerically impossible. To deal with this problem, we give a Monte Carlo method to approximate these bounds. This is evaluated using IEEE 14-bus, 39-bus and 118-bus test systems. In particular, the 118-bus system is tested to demonstrate the scalability of the proposed method.

In this paper, we assume that all the measurements are made using PMUs without SCADA. This is in line with [3–25], which is justified when the PMUs become more readily available and that many traditional measuring devices can be converted into PMU-like devices with GPS-based timing capability. PMU-only based state estimation also has the advantage of fast dynamic response due to the high sampling rate, and this feature is particularly important for power systems involving highly volatile renewable energy sources. We also note that the proposed method can be easily modified to accommodate additional SCADA measurements. Some treatments for mixed PMU and SCADA measurements can be found in [28,29].

The remaining sections of this paper are organized as follows. Both SSE and DSE are introduced in Section 2. Optimization criteria for the two kinds of state estimators are formulated in Section 3. Section 4 gives the modified ILP method and the details of the optimal PMU placement search algorithms. Case studies and analysis are illustrated via simulations based on the IEEE 9-bus, 14-bus, 39-bus and 118-bus systems in Section 5. Section 6 concludes the paper.

2. State estimation in power system

In this section we describe the two state estimation scenarios addressed in this paper, namely, static estimation and dynamic estimation.

2.1. Static State Estimation (SSE)

A PMU is typically able to measure not only the voltage phasor of the node where it is installed, but also the current phasors of all

lines connected to this node. Hence, there is a linear relationship between PMU measurements and the system state variables. Thus, the measurement model is given by

$$z = \Gamma C_l x + v \quad (1)$$

where

$$C_l = \begin{bmatrix} I & O \\ \text{Re}(Y_l) & -\text{Im}(Y_l) \\ O & I \\ \text{Im}(Y_l) & \text{Re}(Y_l) \end{bmatrix}, \quad \Gamma = \begin{bmatrix} \gamma^1 & & & \\ & \gamma^2 & & \\ & & \ddots & \\ & & & \gamma^{2d} \end{bmatrix}$$

with $z \in \mathbb{R}^{2d}$ being the PMU measurement vector, which includes the real part and imaginary part of the measured bus voltage and branch current phasors. d is the number of measurements. The entries of the state vector $x \in \mathbb{R}^{2n}$ are the real part and imaginary part of all the bus voltage phasors. n is the number of buses. We assume that x is known a priori to have a white Gaussian distribution with mean value \bar{x}_p and covariance matrix Σ_p . The measurement matrix $C_l \in \mathbb{R}^{2d \times 2n}$ depends on the chosen PMU locations, hence we use the subscript l to denote different PMU placements. Also, $Y_l \in \mathbb{R}^{b \times n}$ is the branch admittance matrix, where b is the number of current measurements. $I \in \mathbb{R}^{g \times g}$ is the identity matrix with g standing for the number of PMUs, and the entries of $O \in \mathbb{R}^{g \times (2n-g)}$ are all zeros. $v \in \mathbb{R}^{2d}$ is the measurement noise vector, which is assumed to be white and Gaussian with zero mean and covariance matrix Σ_v . The random matrix $\Gamma \in \mathbb{R}^{2d \times 2d}$ models the RCO behavior of the power system (i.e., $\gamma^i = 1$ when the i th measurement is available and 0 otherwise). The binary random variables γ^i are assumed to be independent and identically distributed (i.i.d.), with $p_i = \text{Pr}(\gamma^i = 0)$ being the RCO rate of channel i . We further assume that x and v are uncorrelated.

It is worth to note that the priori knowledge of the state (\bar{x}_p and Σ_p) can be obtained from SCADA measurements, which is a nature way to mix SCADA and PMU measurements.

The MAP estimation criterion is given by [30]

$$\hat{x} = \arg \max_x f(x|z) \quad (2)$$

where $f(x|z)$ denotes the probability density function of x conditioned to the measurement z . In the case of the system (1) and (2) becomes

$$\hat{x} = \arg \min_x \left[(z - \Gamma C_l x)^T \Sigma_v^{-1} (z - \Gamma C_l x) + (x - \bar{x}_p)^T \Sigma_p^{-1} (x - \bar{x}_p) \right] \quad (3)$$

Then, it is straightforward to obtain

$$\hat{x} = \left(C_l^T \Gamma^T \Sigma_v^{-1} \Gamma C_l + \Sigma_p^{-1} \right)^{-1} \left(C_l^T \Gamma^T \Sigma_v^{-1} z + \Sigma_p^{-1} \bar{x}_p \right) \quad (4)$$

Using this, the EEC is given by

$$\Sigma_e = \Sigma_p - \Sigma_p C_l^T \Gamma^T \left(\Sigma_v^{-1} + \Gamma C_l \Sigma_p C_l^T \Gamma^T \right)^{-1} \Gamma C_l \Sigma_p \quad (5)$$

In (5), the EEC Σ_e is a function of the PMU location parameter C_l as well as the RCO parameter Γ . Hence, Σ_e is a random matrix which depends on the PMU locations.

2.2. Dynamic State Estimation (DSE)

The dynamics of generators or load flows in power systems usually can be utilized to describe the system dynamic behaviors. In this paper, considering the high sampling rate of PMU measurement as well as the relatively slow changes of the system, we utilize a generic linear model (6) to describe the dynamic behavior of the system.

$$x_{k+1} = A x_k + B \bar{x} + \omega_k \quad (6)$$

where $x_k \in \mathbb{R}^{2n}$ is the state vector at sample time k , $A \in \mathbb{R}^{2n \times 2n}$ is the transition matrix which relates the states at time k and $k + 1$, $B \in \mathbb{R}^{2n \times 2n}$. It is common to choose $B = I - A$ (where I is the identity matrix) so that $\lim_{k \rightarrow \infty} E(x_k) = \bar{x}(E(\cdot))$ denotes expectation). In this case, the term \bar{x} is regarded as the expected steady-state. The noise $\omega_k \in \mathbb{R}^{2n}$ is a white Gaussian vector random process with zero mean and covariance matrix Σ_ω . We also assume that the initial state x_0 has Gaussian distribution with mean \bar{x}_0 and covariance Σ_{x_0} .

The use of the dynamic model (6) can significantly improve the quality of state estimation. This is due to the fact that the high sampling rate of PMUs makes the adjacent state variables (x_{k+1} and x_k) highly correlated, whereas such correlation is much weaker with SCADA measurements. For example, one may use a simple Brownian motion model:

$$x_{k+1} = x_k + \omega_k$$

which means that the state evolves as a random walk, or

$$x_{k+1} = A x_k + (I - A) \bar{x} + \omega_k$$

with $A = \text{diag}\{\alpha_1, \alpha_2, \dots\}$ and $0 < \alpha_i < 1$ for all i , which means the state has tendency to revert back to its steady state \bar{x} .

The measurement model is given by

$$z_k = \Gamma_k C_l x_k + v_k \quad (7)$$

All the parameters in (7) are the same to those in (1), except for the time subscript k .

The estimation of the state in (6) and (7) is carried out using a Kalman filter [31].

$$\begin{aligned} \hat{x}_{k|k} &= \hat{x}_{k|k-1} + G_k [z_k - \Gamma_k C_l \hat{x}_{k|k-1}] \\ \hat{x}_{k+1|k} &= A \hat{x}_{k|k} + B \bar{x} \\ G_k &= \Sigma_{k|k-1} C_l^T \Gamma_k^T (\Gamma_k C_l \Sigma_{k|k-1} C_l^T \Gamma_k^T + \Gamma_k \Sigma_v \Gamma_k^T)^{-1} \\ \Sigma_{k|k} &= \Sigma_{k|k-1} - G_k \Gamma_k C_l \Sigma_{k|k-1} \Sigma_{k+1|k} = A \Sigma_{k|k} A^T + \Sigma_\omega, \end{aligned} \quad (8)$$

which is initialized by $\Sigma_{0-1} = \Sigma_{x_0}$ and $\hat{x}_{0-1} = \bar{x}_0$. The variable $\hat{x}_{k|k-1}$ denotes the prediction of the state at time instant k , based on the measurements available up to time $k - 1$, and $\Sigma_{k|k-1}$ denotes its associated error covariance. Then, $\hat{x}_{k|k-1}$ and $\Sigma_{k|k-1}$ are used as the prior statistical information of the state, to build its estimate $\hat{x}_{k|k}$ at time k , once the measurement at time k becomes available. The auxiliary matrix G_k is called the Kalman gain.

Remark 1. If the parameters A , B and Σ_ω in (6) or Σ_v in (7) are not available, they can be identified either offline or online. SCADA measurements are particularly suitable for carrying out this task, due to their high redundancy [32]. This identification problem is not considered in this paper.

3. Optimization criterion for PMU placement

The stochastic nature of RCOs turns the EEC into random matrices in both SSE and DSE cases. As explained in Section 1, the natural criterion for choosing the PMU locations is to minimize the expected EEC norm $E(\|\Sigma_e\|)$, in the SSE case, and the asymptotic expected EEC norm $\lim_{k \rightarrow \infty} E(\|\Sigma_{k|k}\|)$, in the DSE case. The norm $\|\cdot\|$ denotes the largest eigenvalue of the matrix. For SSE, it is relatively simple to calculate $E(\|\Sigma_e\|)$. However, for DSE, a difficulty arises because there is no exact expression for computing $\lim_{k \rightarrow \infty} E(\|\Sigma_{k|k}\|)$. However, it turns out that we can still find the optimal locations by using a sequence of lower and upper bounds for this limit. We describe below the resulting optimization criteria for both SSE and DSE. Finally, Monte Carlo methods are given to simplify the calculations of the optimization procedures.

3.1. Optimization criterion for SSE

Recall that g denotes the number of PMU measurements. Let $S_m \in \mathbb{R}^{2d \times 2d}$, $m = 1, \dots, 2^g$ denote all 2^g possible measurement arrival patterns at each time instant. Let $\Pr(S_m)$ be the probability that $\Gamma = S_m$. Then the expected EEC norm $E(\|\Sigma_e\|)$ of SSE (4) can be computed by

$$E(\|\Sigma_e\|) = \sum_{m=1}^{2^g} \Pr(S_m) \|\Sigma_e\| \quad (9)$$

where Σ_e given by (5).

3.2. Optimization criterion for DSE

Instead of calculating the asymptotic expected EEC norm $\lim_{k \rightarrow \infty} E(\|\Sigma_{k|k}\|)$, a sequence of monotonically tight upper and lower bounds are proposed for DSE.

3.2.1. Upper and lower bounds

The next lemma introduces the starting point for obtaining the sequence of monotonically tight upper and lower bounds.

Lemma 1. *Let*

$$\begin{aligned} \underline{\Sigma} &= \text{sol}_{\Sigma} \left\{ \Sigma = A\Sigma A' + \Sigma_{\omega} - A\Sigma C_l'(C_l\Sigma C_l' + \Sigma_v)^{-1} C_l\Sigma A' \right\} \\ \bar{\Sigma} &= \text{sol}_{\Sigma} \left\{ \Sigma = A\Sigma A' + \Sigma_{\omega} \right\} \end{aligned}$$

Then, if $\Sigma_0 \geq \underline{\Sigma}$, for all k ,

$$\underline{\Sigma} \leq \Sigma_k \leq \bar{\Sigma} \quad (10)$$

Proof. Notice that $\underline{\Sigma}$ is the steady state solution for the standard Kalman filtering problem when no packet drop occurs, and $\bar{\Sigma}$ is the same solution obtained when all the measurement are lost. \square

The bounds in Lemma 1 are too loose to be used for our optimization problem. Below we explain how they can be refined to make them arbitrarily tight, at the expense of increased computational.

Let G_k^N describe the measurements received from time $k - N$ to $k - 1$, i.e.,

$$G_k^N = \{\Gamma_{k-N+1}, \Gamma_{k-N+2}, \dots, \Gamma_{k-1}\} \quad (11)$$

Also, we let S_m^N , $m = 1, \dots, 2^{Ng}$ denote all 2^{Ng} possible arrival patterns in a time interval of length N . Let $\Pr(S_m^N)$ be the probability that $G_k^N = S_m^N$, i.e., that the sequence S_m^N was observed from times $k - N$ to $k - 1$. Also, let $\phi(\cdot, \cdot)$ be the function describing the evolution of the error covariance according to a given sequence, i.e., $\Sigma_k = \phi(\Sigma_{k-N}, G_k^N)$. Then, we define

$$\begin{aligned} \underline{C}_N &= \sum_{m=1}^{2^{Ng}} \Pr(S_m^N) \|\phi(\underline{\Sigma}, S_m^N)\| \\ \bar{C}_N &= \sum_{m=1}^{2^{Ng}} \Pr(S_m^N) \|\phi(\bar{\Sigma}, S_m^N)\| \end{aligned} \quad (12)$$

The next lemma shows that \underline{C}_N is monotonically increasing and \bar{C}_N is monotonically decreasing.

Lemma 2.

$$\begin{aligned} \underline{C}_{N+1} &< \underline{C}_N \\ \bar{C}_{N+1} &> \bar{C}_N \end{aligned} \quad (13)$$

Proof. We will only show the monotonicity of the lower bound. That of the upper bound follows from the same argument. Consider the following partition of the sequence S_j^{N+1} :

$$S_j^{N+1} = \{S_n^1, S_m^N\} \quad (14)$$

Then,

$$\begin{aligned} \underline{C}_{N+1} &= \sum_{m=1}^{2^{Ng}} \sum_{n=1}^{2^g} \Pr(S_m^N) \Pr(S_n^1) \|\phi(\underline{\Sigma}, \{S_n^1, S_m^N\})\| \\ &= \sum_{m=1}^{2^{Ng}} \Pr(S_m^N) \sum_{n=1}^{2^g} \Pr(S_n^1) \|\phi(\underline{\Sigma}, S_n^1, S_m^N)\| \\ &\geq \sum_{m=1}^{2^{Ng}} \Pr(S_m^N) \|\phi(\underline{\Sigma}, S_m^N)\| = \underline{C}_N \end{aligned} \quad (15)$$

where the inequality in (15) follows since

$$\phi(\underline{\Sigma}, S_n^1) \geq \underline{\Sigma} \quad (16)$$

\square

Now, it follows from [33, Theorem 2.4] that the bounds \underline{C}_N and \bar{C}_N approach the asymptotic expected norm of the error covariance as $N \rightarrow \infty$, i.e.,

$$\begin{aligned} \lim_{N \rightarrow \infty} \underline{C}_N &= \lim_{k \rightarrow \infty} E(\|\Sigma_k\|) \\ \lim_{N \rightarrow \infty} \bar{C}_N &= \lim_{k \rightarrow \infty} E(\|\Sigma_k\|) \end{aligned} \quad (17)$$

Hence, from Lemma 2, we have that

$$\underline{C}_N \leq E(\|\Sigma_k\|) \leq \bar{C}_N \quad (18)$$

i.e., \underline{C}_N and \bar{C}_N are bounds on $\lim_{k \rightarrow \infty} E(\|\Sigma_k\|)$, which become monotonically tight at the limit.

3.3. Monte Carlo approximation

The numbers of possible arrival patterns, i.e. 2^g for SSE and 2^{Ng} for DSE will become extremely large when the size of system increases. Hence, to simplify the calculation of the optimization criteria. We use the following Monte Carlo approximations.

3.3.1. Criterion approximation for SSE

$$\tilde{E}(\|\Sigma_e\|) = \frac{1}{M} \sum_{i=1}^M \|\Sigma_e\|_{S_i} \quad (19)$$

where S_i , $i = 1, 2, \dots, M$ stand for the different realizations of random measurement arrival patterns, M is the number of realizations.

3.3.2. Criterion approximation for DSE

$$\begin{aligned} \tilde{C}_N &= \frac{1}{M} \sum_{i=1}^M \|\phi(\underline{\Sigma}, S_i^N)\| \approx \underline{C}_N \\ \tilde{\bar{C}}_N &= \frac{1}{M} \sum_{i=1}^M \|\phi(\bar{\Sigma}, S_i^N)\| \approx \bar{C}_N \end{aligned} \quad (20)$$

where S_i^N , $i = 1, 2, \dots, M$ are M realizations of random measurement arrival patterns till time N .

It is noted that the number M of realizations needs to be sufficiently large so that the approximation error is small. According to our tests, $M = 5000$ is typically sufficient for both cases.

4. Optimal PMU placement algorithm

In both SSE and DSE, we need to find the optimal PMU placements in the sense of minimizing either $E(\|\Sigma_e\|)$ or $\lim_{k \rightarrow \infty} E(\|\Sigma_{k|k}\|)$. In principle, this could be done evaluating these magnitudes for all possible PMU arrangements. However, this can be numerically

unaffordable in a large power network. Hence, to reduce the numerical complexity, the initial set of candidates is formed by those PMU arrangements which result in systems being topologically observable. This can be done using any available method. In this sense, the optimal PMU placement algorithm contains two main steps: (1) candidate PMU placement solutions calculation and (2) state estimation performance refining.

4.1. Candidate PMU placement solutions calculation

In this paper the ILP method proposed in [16] is chosen and modified to search for candidate PMU placements. The original ILP method is valid to get a PMU placement solution which can make the whole system topologically observable with minimum number of PMUs. However, this method gives only one such possible solution. Hence, we propose a modified version where an auxiliary parameter is introduced, which can excite all the possible PMU placement solutions with a sufficiently large number of realizations. In the modified version, we also consider the MMR criterion proposed in [5,15,23,22]. According to our simulation results, although the MMR criterion can not lead to a unique solution, it is still useful to refine the original set of candidate solutions, especially for relatively large power systems. We will also modify the ILP method to allow some redundancy in the PMU number, which is useful in making state estimation robust and fault tolerant.

4.1.1. The original ILP method

We first roughly review the original ILP method in [16], as follows:

$$s_{PMU} = \min \sum_{i=1}^n u_i \quad (21)$$

s.t. $T_{PMU}U \geq b$

where T_{PMU} is a binary connectivity matrix (see the details in [16]), $b = [1, 1, \dots, 1]_{n \times 1}^T$. $U = [u_1, u_2, \dots, u_n]^T$, where $u_i \in \{0, 1\}$ is the PMU placement variable on the i th bus, with 0 indicating no placement and 1 indicating a placement. Based on the above ILP method, we can obtain the minimum number of PMU, i.e. s_{PMU} , that is necessary for topological observability. Take $\tilde{s}_{PMU} \geq s_{PMU}$ to allow some possible redundancy, if necessary.

4.1.2. Modified version of ILP

(i) Without MMR criterion

An auxiliary parameter $D = [d_1, d_2, \dots, d_n]$, $d_i = \text{rand}(0, 1)$, $i = 1, 2, \dots, n$, is added in the cost function. When the number of realizations of D is sufficiently large, all the possible of candidate optimal PMU placement solutions will be generated. A new constraint is added to guarantee the required number of PMUs, as follows:

$$\begin{aligned} \min \quad & DU \\ \text{s.t.} \quad & T_{PMU}U \geq b \\ & \sum_{i=1}^n u_i = \tilde{s}_{PMU} \end{aligned} \quad (22)$$

(ii) With MMR criterion

We first calculate the maximum number of measurements, m_{PMU} , of \tilde{s}_{PMU} PMUs via:

$$\begin{aligned} m_{PMU} = \max \quad & \sum_{i=1}^n u_i |T_{PMU,i}| \\ \text{s.t.} \quad & T_{PMU}U \geq b \\ & \sum_{i=1}^n u_i = \tilde{s}_{PMU} \end{aligned} \quad (23)$$

where $|T_{PMU,i}|$ stands for the number of 1's in the i th row of T_{PMU} . Then use the following ILP method to generate all the possible candidate optimal PMU placement solutions, which guarantee topological observability with \tilde{s}_{PMU} PMUs and contain m_{PMU} measurements.

$$\begin{aligned} \min \quad & DU \\ \text{s.t.} \quad & T_{PMU}U \geq b \\ & \sum_{i=1}^n u_i = \tilde{s}_{PMU} \\ & \sum_{i=1}^n u_i |T_{PMU,i}| = m_{PMU} \end{aligned} \quad (24)$$

4.2. State estimation performance refining

After the candidate set of optimal PMU placement solutions are obtained, state estimation performance, EEC, is used as the final optimization criterion to choose the best placement solution.

For SSE, the expected EEC norm $E(\|\Sigma_e\|)$ for each candidate solution is directly evaluated using (9). Then the optimal solution is chosen as the one with the smallest $E(\|\Sigma_e\|)$.

For DSE, we use the bounds \underline{C}_N and \overline{C}_N to derive an algorithm for finding the optimal PMU placements in the sense of minimizing $\lim_{k \rightarrow \infty} E(\|\Sigma_{k|k}\|)$. In principle, this could be done by choosing N large enough so that both bounds are "sufficiently close". However, this approach can be numerically unaffordable since the complexity of evaluating \underline{C}_N and \overline{C}_N grows exponentially with N or g . To avoid this, we propose an alternative algorithm. The main idea is to proceed sequentially for $N = 1, 2, \dots$. For each N , the bounds \underline{C}_N and \overline{C}_N are computed for all candidate PMU arrangements (i.e., the initial set of candidate arrangements). Then, all arrangements whose lower bound is greater than the smallest upper bound between all candidate arrangements, is eliminated from the set of candidates, before continuing to the next step. The steps proceed until only one candidate is left. We summarize these steps below:

- Set $N = 1$ and obtain the initial set of candidate solutions. To this end we use the modified ILP algorithm proposed above.
- Compute the upper bound \overline{C}_N for all candidate solution and let \overline{C}_N be the smallest among them.
- For each candidate solution compute the lower bound \underline{C}_N , and if this value is greater than \overline{C}_N , remove the solution from the set of candidates.
- If the set of candidates has only one solution, stop the iterations; otherwise, put $N = N + 1$ and go to (b).

Remark 2. For large power systems, a combination of the proposed algorithm and the Monte Carlo approximation will be a good choice to optimize the PMU placement solutions, which will be tested on the IEEE 39-bus and 118-bus system later.

5. Simulation results

The performance of the proposed SSE and DSE estimators are evaluated on the IEEE 9-bus (shown in Fig. 1), 14-bus, 39-bus and 118-bus test systems separately (the topological structure of the last three standard IEEE test systems can be found in [34]). The optimal PMU placement solution is obtained by comparing the corresponding SE performances.

Since the size of the power system does not affect the calculation speed of SSE performance (19) seriously, the test procedures for the four systems are similar. Hence SSE is tested for the IEEE 9-bus system only.

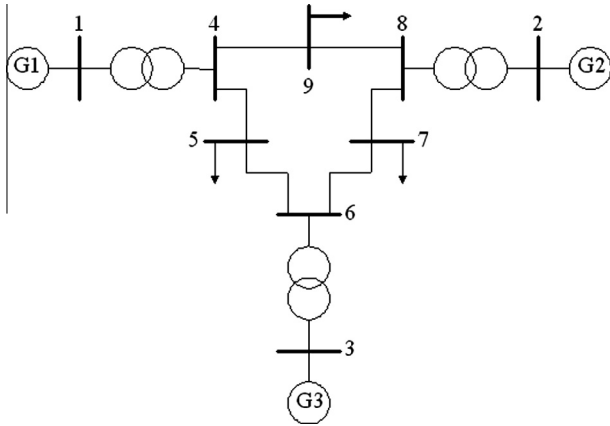


Fig. 1. The topological structure of IEEE 9-bus system.

For DSE, the IEEE 9-bus system is used to test the original upper and lower bounds in (12). The Monte Carlo approximations of the upper and lower bounds in (20) are tested by the IEEE 14-bus system. Finally, the Monte Carlo approximation method is used to choose the best PMU placement solutions for the IEEE 39-bus and 118-bus systems. In all simulations, we take $\tilde{s}_{PMU} = s_{PMU}$ for simplicity.

5.1. IEEE 9-bus system

To obtain the initial set of candidate solutions in the IEEE 9-bus system, we use the modified LIP algorithm (22), which gives all PMU arrangements leading to topologically observable systems, using the minimum number of PMUs. The resulting set has four solutions, each of them using three PMUs. The installation buses of these four solutions are {1, 6, 8}, {2, 4, 6}, {3, 4, 8} and {4, 6, 8}, respectively. We point out that the solution {4, 6, 8} has two extra current measurements, in comparison with the other three solutions. This makes the comparison somehow unfair, since this solution consumes more communication resources than the others. Hence, we remove two current measurements on Branch 5 and 9 from the fourth solution so that all solutions have the same number of measurements. It is noted that without the two current measurements, the fourth solution still can make the system topologically observable.

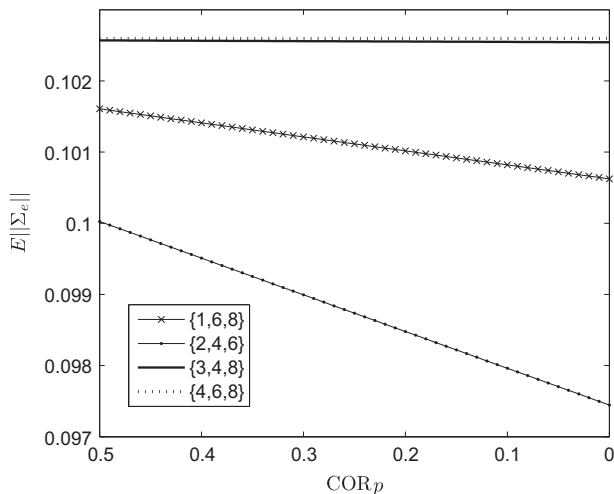


Fig. 2. $E(\|\Sigma_e\|)$ of four candidate locations in IEEE 9-bus system.

Table 1
Simulation values of parameters of IEEE 9-bus system.

A	$diag(0.8, 0.8, 0.95, 0.8, 0.95, 0.95, 0.8, 0.95, 0.8)$
B	$diag(0.2, 0.2, 0.05, 0.2, 0.05, 0.05, 0.2, 0.05, 0.2)$
Σ_ω	$diag(0.1^2, \dots, 0.1^2)$
Σ_v	$diag(0.1^2, \dots, 0.1^2)$
Σ_{x_0}	$diag(0.1^2, \dots, 0.1^2)$

We assume that RCO affects all the measurements of a PMU simultaneously. In other words, when RCO occurs, all the measurements of the corresponding PMU will be lost. Hence, there are 2^3 and 2^{3N} received measurement patterns for SSE and DSE, respectively. This assumption is not necessary for the proposed method, and is used only to simplify the computation.

5.1.1. Static estimation

The static measurement model (1) is summarized by the data given by IEEE 9-bus system, with $\Sigma_v = diag(0.1^2, \dots, 0.1^2)$. Fig. 2 shows the estimation performance, i.e., $E(\|\Sigma_e\|)$, of the four candidate optimal locations, with p varying from 0.5 to 0. From this figure, we can see that the placement {3, 4, 8} always has the best estimation performance for different CORs.

5.1.2. Dynamic estimation

The associated dynamical system model (6) and (7) used in our simulation is summarized in Table 1. This particular set of values used here is just an example to test the proposed method.

To illustrate the convergence of the bounds \underline{C}_N and \overline{C}_N we show in Figs. 3 and 4 their values for different values of N , corresponding to the fourth solution {4, 6, 8}. The packet loss rates are 0.05 and 0.35 respectively. We can see how both bounds converge monotonically to the same limit value and that the converging speed changes for a different RCO rate.

The bounds for the four candidate solutions for packet loss rates of 0.05 and 0.35 are shown in Figs. 5 and 6 respectively. From the two figures, we can see the following: (1) The optimal PMU placement solutions for both cases can be found after four iterations. Even the gaps between the upper bound and the lower bound shown in Figs. 3 and 4 are still distinct at sample time four, the optimal solution can be already identified. (2) The optimal solutions depend on the packet loss rate. For different packet loss rates,

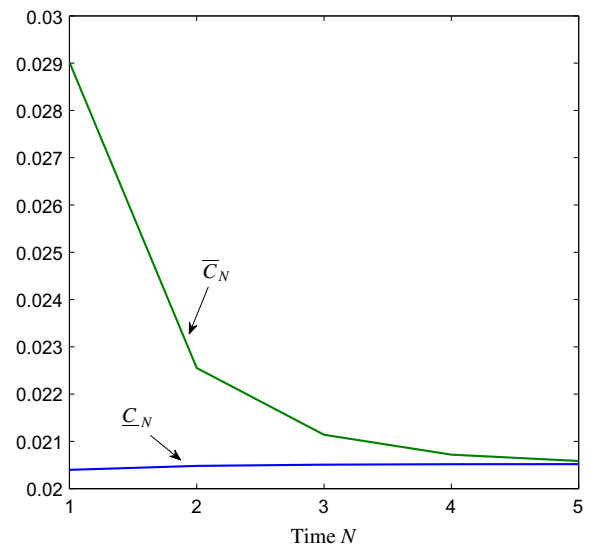


Fig. 3. Bounds of $\lim_{k \rightarrow \infty} E(\|\Sigma_k\|)$ in IEEE 9-bus system, PMUs located in buses {4, 6, 8}, $p_i = 0.05$.

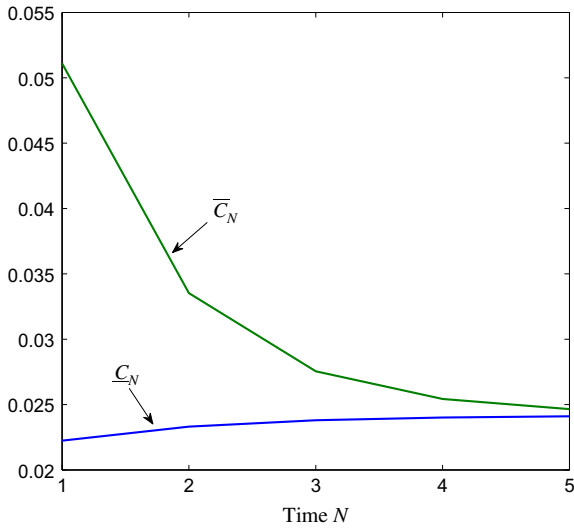


Fig. 4. Bounds of $\lim_{k \rightarrow \infty} E(\|\Sigma_k\|)$ in IEEE 9-bus system, PMUs located in buses {4,6,8}, $p_i = 0.35$.

the final solution switches between the second candidate solution {2,4,6} and the third one {3,4,8}.

5.2. IEEE 14-bus system

There are five candidate PMU placement solutions in the IEEE 14-bus system, i.e., {2,6,7,9}, {2,6,8,9}, {2,7,10,13}, {2,7,11,13}, {2,8,10,13}. The solution {2,6,7,9} is used to examine how the Monte Carlo approximation (20) works. Fig. 7 shows the simulation results, from which we can see that with $M = 5000$, the upper and lower bounds can be approximated well for different values of N . The best PMU placement solution obtained via (20) is {2,6,7,9}. The details of the search result is shown in Table 2.

5.3. IEEE 39-bus and 118-bus systems

In order to test the scalability of the proposed method for large size power systems, the IEEE 39-bus and 118-bus systems are

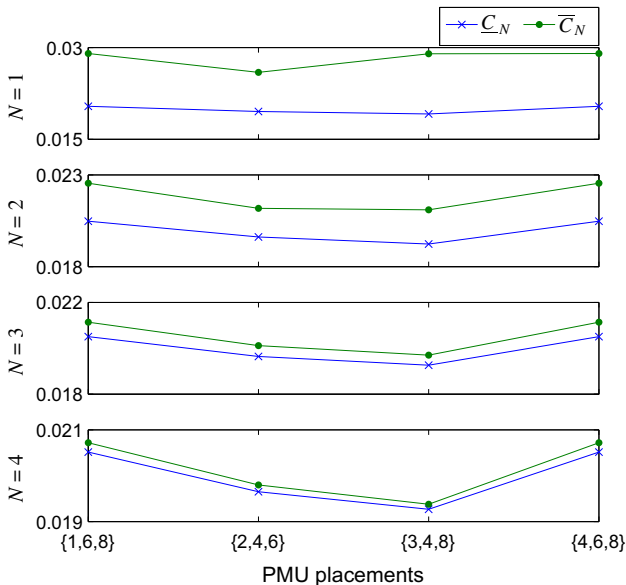


Fig. 5. Bounds of $\lim_{k \rightarrow \infty} E(\|\Sigma_k\|)$ in IEEE 9-bus system, $p_i = 0.05$.

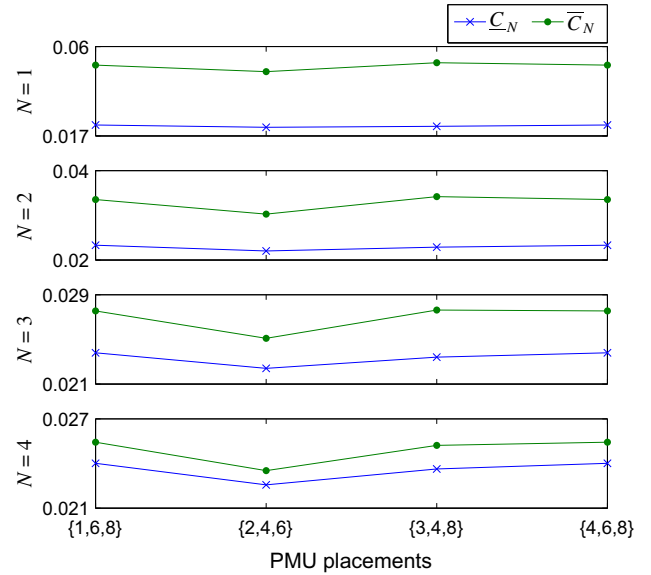


Fig. 6. Bounds of $\lim_{k \rightarrow \infty} E(\|\Sigma_k\|)$ in IEEE 9-bus system, $p_i = 0.35$.

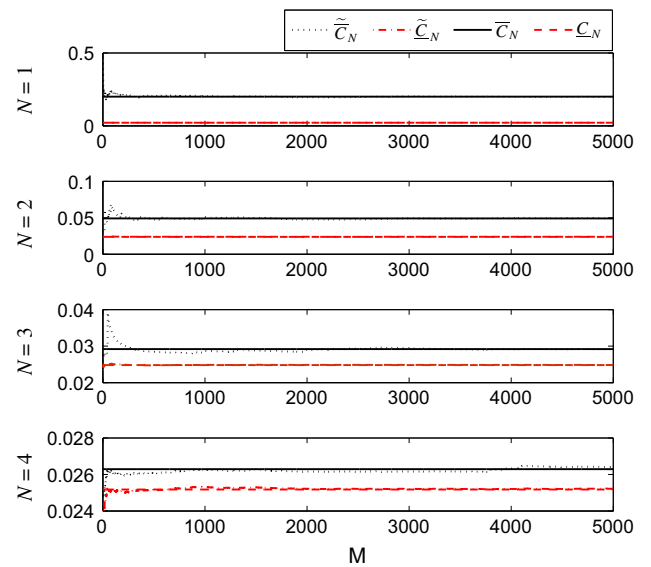


Fig. 7. Monte Carlo approximations in IEEE 14-bus system, $p = 0.1$

Table 2 Searching progress of the optimal PMU placement algorithm.

Time N	Number of candidate solutions left								
	1	2	3	4	5	6	7	8	9
14-Bus	5	5	5	3	2	1	N/A	N/A	N/A
39-Bus	48	48	48	40	8	8	7	2	1
118-Bus	78	78	78	12	10	2	2	2	1

studied. The modified ILP algorithm with MMR criterion (24) is used for the IEEE 39-bus and 118-bus systems respectively, then 48 and 78 candidate PMU placement solutions are found. Monte Carlo approximations \tilde{C}_N and \bar{C}_N are calculated for different candidate solutions with $M = 5000$. Table 2 shows the search result. The IEEE 39-bus system get its best PMU placement solution {2,6,9,10,11,14,17,19,20,22,23,25,29} (using 13 PMUs). The

solution {3,5,9,12,15,17,21,25,28,34,37,40,45,49,53,56,62,64,68,70,71,76,79,85,86,89,92,96,100,105,110,114} (using 32 PMUs) is found to be the best for the IEEE 118-bus system.

6. Conclusion

In this paper, a new method is proposed for optimal PMU placement in power systems suffering from random component outages. The state estimation performances of two kinds of estimators (i.e., SSE and DSE) are evaluated based on different PMU locations and different RCO rates. Then using the norm of the estimation error covariance as the optimization criterion, an algorithm is proposed to solve the optimization problem. This method chooses the placement from a set of candidate PMU placements, each of them guaranteeing topological observability. Then the optimal PMU placement is chosen to minimize the expected value and the asymptotic expected value of the norm of the state estimation error covariance for SSE and DSE, respectively. In view of the potential difficulty in computation, we propose a sequential algorithm which uses a sequence of lower and upper bounds for the estimation error covariance, which are monotonically tight. The proposed method is tested on several standard IEEE test systems. The simulation results show the validity of the proposed algorithm to deal with the RCO problem. Finally, we note that the optimal PMU placement in general depends on power network topology and system parameters. Since placement is typically done at planning stage, the most representative system model should be used for searching the optimal PMU placement. Further research is needed to seek robust PMU placements under different operating conditions (including normal and faulty conditions).

References

- [1] Schweppe FC, Wildes J. Power system static-state estimation, part I, II, III. *IEEE Trans Power Apparatus Syst*, PAS-89 1970(1):120–35.
- [2] Ree JDL, Centeno V, Thorp JS, Phadke AG. Synchronized phasor measurement applications in power systems. *IEEE Trans Smart Grid* 2010;1(1):20–7.
- [3] Baldwin TL, Mili L, Boisen MJB, Adapa R. Power system observability with minimal phasor measurement placement. *IEEE Trans Power Syst* 1993;8(2):707–15.
- [4] Nuqui RF, Phadke AG. Phasor measurement unit placement techniques for complete and incomplete observability. *IEEE Trans Power Deliv* 2005;20(4):2381–8.
- [5] Milosevic B, Begovic M. Nondominated sorting genetic algorithm for optimal phasor measurement placement. *IEEE Trans Power Syst* 2003;18(1):69–75.
- [6] Aminifar F, Lucas C, Khodaei A, Fotuhi-Firuzabad M. Optimal placement of phasor measurement units using immunity genetic algorithm. *IEEE Trans Power Deliv* 2009;24(3):1014–20.
- [7] Peng C, Sun H, Guo J. Multi-objective optimal PMU placement using a non-dominated sorting differential evolution algorithm. *Int J Electr Power Energy Syst* 2010;32(8):886–92.
- [8] Jamuna K, Swarup KS. Optimal placement of PMU and SCADA measurements for security constrained state estimation. *Int J Electr Power Energy Syst* 2011;33(10):1658–65.
- [9] Cho K-S, Shin J-R, Hyun SH. Optimal placement of phasor measurement units with GPS receiver. In: *IEEE power engineering society winter meeting*; 2011. p. 258–62.
- [10] Peng J, Sun Y, Wang HF. Optimal PMU placement for full network observability using Tabu search algorithm. *Int J Electr Power Energy Syst* 2006;28(4):223–31.
- [11] Chakrabarti S, Kyriakides E. Optimal placement of phasor measurement units for power system observability. *IEEE Trans Power Syst* 2008;23(3):1433–40.
- [12] Hurtgen M, Maun JC. Optimal PMU placement using iterated local search. *Int J Electr Power Energy Syst* 2010;32(8):857–60.
- [13] Ahmadi A, Alinejad-Beromi Y, Moradi M. Optimal PMU placement for power system observability using binary particle swarm optimization and considering measurement redundancy. *Expert Syst Appl* 2011;38(6):7263–9.
- [14] Mahdi H, Mohammad RA, Amraee MT, Babak. Optimal placement of PMUs to maintain network observability using a modified BPSO algorithm. *Int J Electr Power Energy Syst* 2011;33(1):28–34.
- [15] Dua D, Dambhare S, Gajbhiye RK, Soman SA. Optimal multistage scheduling of PMU placement: an ILP approach. *IEEE Trans Power Deliv* 2008;23(4):1812–20.
- [16] Gou B. Optimal placement of PMUs by integer linear programming. *IEEE Trans Power Syst* 2008;23(3):1525–6.
- [17] Gou B. Generalized integer linear programming formulation for optimal PMU placement. *IEEE Trans Power Syst* 2008;23(3):1099–104.
- [18] Aminifar F, Khodaei A, Fotuhi-Firuzabad M, Shahidehpour M. Contingency-constrained PMU placement in power networks. *IEEE Trans Power Syst* 2010;25(1):516–23.
- [19] Azizi S, Dobakhshari AS, Sarmadi SAN, Ranjbar AM. Optimal PMU placement by an equivalent linear formulation for exhaustive search. *IEEE Trans Smart Grid* 2012;3(1):174–82.
- [20] Enshaei A, Hooshmand RA, Fesharaki FH. A new method for optimal placement of phasor measurement units to maintain full network observability under various contingencies. *Electric Power Syst Res* 2012;89(0):1–10.
- [21] Chakrabarti S, Eliades D, Kyriakides E, Albu M. Measurement uncertainty considerations in optimal sensor deployment for state estimation. In: *IEEE international symposium on intelligent signal processing*; 2007. p. 1–6.
- [22] Chakrabarti S, Kyriakides E, Eliades DG. Placement of synchronized measurements for power system observability. *IEEE Trans Power Deliv* 2009;24(1):12–9.
- [23] Peng C, Xu X. A hybrid algorithm based on BPSO and immune mechanism for PMU optimization placement. In: *7th World congress on intelligent control and automation*; 2008. p. 7036–40.
- [24] Zhang J, Welch G, Bishop G, Huang Z. Optimal PMU placement evaluation for power system dynamic state estimation. In: *Innovative smart grid technologies conference Europe (ISGT Europe)*; 2010. p. 1–7.
- [25] Aminifar F, Fotuhi-Firuzabad M, Shahidehpour M, Khodaei A. Observability enhancement by optimal PMU placement considering random power system outages. *Energy Syst* 2011;2:45–65.
- [26] Chawasak R, Suttichai P, Sermsak U, Neville RW. An optimal PMU placement method against measurement loss and branch outage. *IEEE Trans Power Deliv* 2007;22(1):101–7.
- [27] Roy BKS, Sinha AK, Pradhan AK. An optimal PMU placement technique for power system observability. *Int J Electr Power Energy Syst* 2012;42(1):71–7.
- [28] Zivanovic R, Cairns C. Implementation of PMU technology in state estimation: an overview. In: *IEEE 4th AFRICON*; 1996. p. 1006–11.
- [29] Jamuna K, Swarup KS. Two stage state estimator with phasor measurements. In: *International conference on power systems*; 2009. p. 1–5.
- [30] Steven MK. *Fundamentals of statistical signal processing*. NJ (USA): Prentice Hall; 1993.
- [31] Anderson BDO, Moore JB. *Optimal filtering*. Mineola (NY): Dover Publications, Inc.; 1979.
- [32] Indulkar C, Ramalingam K. Estimation of transmission line parameters from measurements. *Int J Electr Power Energy Syst* 2008;30(5):337–42.
- [33] Bougerol P. Kalman filtering with random coefficients and contractions. *SIAM J Control Optim* 1993;31:942–59.
- [34] Standard IEEE test system. <<http://www.ee.washington.edu/research/pstca>>.